

Tunable-focus microlens arrays on curved surfaces

Difeng Zhu, Chenhui Li, Xuefeng Zeng, and Hongrui Jiang^{a)}

Department of Electrical and Computer Engineering, University of Wisconsin-Madison, Madison, Wisconsin 53706, USA

(Received 18 December 2009; accepted 3 February 2010; published online 25 February 2010)

We present a microlens array consisting of multiple liquid-based tunable-focus microlenses omnidirectionally fabricated on a hemisphere, resulting in large field of view. Polymer bridge structure is formed between microlenses to reduce the stress and deformation in each lens structure. Each microlens in the array is formed via a water-oil interface at its lens aperture. Photopatterned thermo-responsive hydrogel actuators are used to regulate the curvature of the water-oil interface, thus tuning the focal length, ranging from millimeters to infinity. © 2010 American Institute of Physics. [doi:10.1063/1.3330965]

Optical imaging and microscopy are extensively used in biomedical, industrial, and military applications, and there is a continuing trend in the miniaturization of such systems.¹⁻⁴ Microlenses are critical in these systems. However, traditional microlenses and microlens arrays suffer narrow field of view (FOV).^{5,6} To address this issue, it is desirable to make microlens arrays onto curvilinear surfaces, like compound eyes of insects.^{5,7} Nevertheless, conventional fabrication methods are planar in nature. Although there are curvilinear fabrication processes developed, they are generally very complicated.^{6,8,9} Furthermore, most microlens arrays are made with fixed focus,^{10,11} which would significantly restrict the optical information acquired.

Here, we present a liquid-based microlens array omnidirectionally fabricated on a glass hemispherical dome for large FOV. Each lens can be tuned in focal length individually, resulting in high spatial resolution. The tuned focal lengths of the microlens array range from millimeters to infinity. Thermo-responsive hydrogel is used for tuning, which avoids the requirement of complicated actuation systems.^{12,13} The microlenses are connected through thin polymer bridge structures to reduce the stress and thus the deformation in the microlens array. The whole fabrication process is relatively simple.

Figure 1(a) shows the three-dimensional schematics of one liquid tunable-focus microlens in an array fabricated on a hemispherical dome. A polymer cavity, consisting of a substrate, a polymer slip defining the aperture, and a hydrogel actuator, is filled with water. Silicone oil covers onto water to prevent the evaporation and serves as the lens material since its refractive index (1.48) is higher than that of water (1.33). The sidewall of the aperture slip is treated hydrophilic while the top surface of the aperture slip is naturally hydrophobic.^{12,13} Thus, a water-oil meniscus, whose circumference is pinned by a hydrophobic-hydrophilic (H-H) boundary at the top edge of the aperture, functions as a microlens. Thermo-responsive reversible N-isopropylacrylamide (NIPAAm) hydrogel serves as the actuator to tune the focal length of the microlens. As the temperature decreases (increases), the hydrogel swells (contracts), regulating the curvature of the water-oil meniscus.

The water-oil interface protrudes upward at low temperatures (divergent), and bulges downward at high temperatures (convergent), as shown in Fig. 1(a). Therefore, the focal length of this liquid microlens is varied. Figure 1(b) are photoimages of a microlens in two statuses: divergent and convergent. The left image (divergent) was taken at around 50 °C, while the

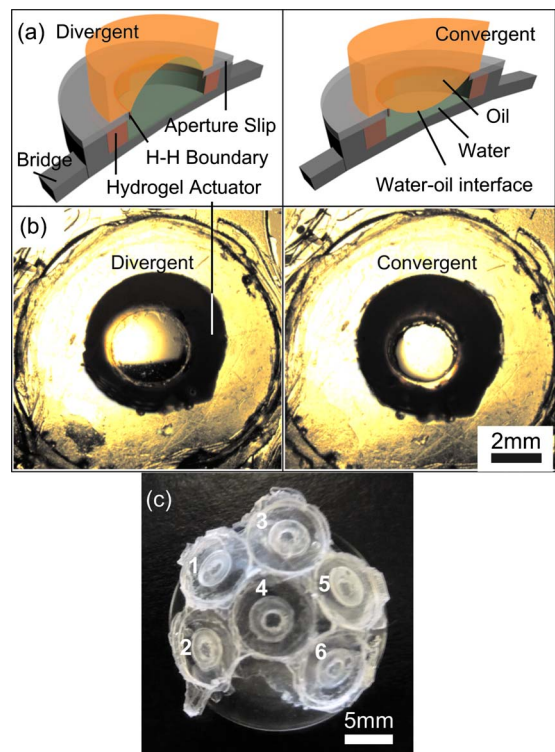


FIG. 1. (Color online) (a) Schematics of one microlens structure in divergent and convergent statuses, respectively. A round PDMS slip defining the lens aperture, a hydrogel actuator and the underlying polymer substrate form a water container. The sidewalls of the aperture are chemically treated hydrophilic by corona plasma discharge, while the top surfaces are naturally hydrophobic. A meniscus, used as a microlens, is formed through a curved interface between water and oil and is pinned by the H-H boundary, protruding upward at high pressure (divergent) and bulging downward at low pressure (convergent). (b) Photoimages of a microlens in the two statuses: divergent and convergent. The left image (divergent) was taken at around 50 °C; the right image (convergent) was taken at about 30 °C. The scale bar is 2 mm. (c) Image of a six-element microlens array on a dome with a diameter of 18 mm. Each microlens is labeled with a number. The scale bar is 5 mm.

^{a)} Author to whom correspondence should be addressed. Tel.: 608-265-9418, FAX: 608-262-1267. Electronic mail: hongrui@engr.wisc.edu.

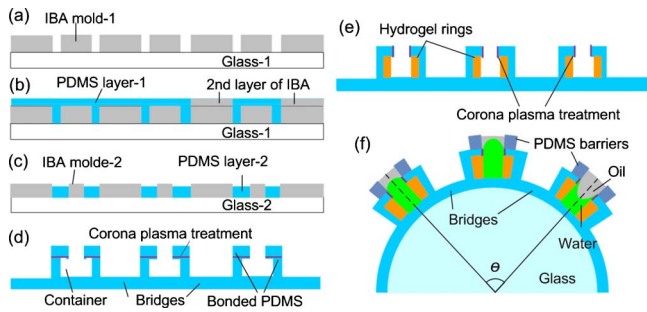


FIG. 2. (Color online) Fabrication process flow of a tunable-focus microlens array fabricated on a glass hemisphere. (a) An IBA layer was initially photopatterned on a glass slide. (b) The heightened IBA layer served as a mold for PDMS substrate with bridges. (c) Another IBA mold was photopatterned on the second glass slide for PDMS aperture layer. (d) The cavities were formed by bonding two treated PDMS layers together. (e) NIPAAm hydrogel rings were photopatterned in the cavities as actuators. The sidewall of the aperture slip was treated from hydrophobic to hydrophilic to pin the water-oil meniscus. (f) A water and oil interface was formed at the edge of each aperture slip, serving as a lens. The microlens array was wrapped onto a hemispherical dome and was distributed on a cap. θ is defined as the angle that this cap subtends. A separately fabricated round PDMS barrier (fabrication process not shown here) was placed onto each microlens to keep oil in the package.

right image (convergent) was taken at about 30 °C.

After a planar tunable-focus microlens array is fabricated, it is wrapped onto a hemispherical dome with a diameter of 18 mm, as shown in Fig. 1(c). When a planar substrate is wrapped onto a hemispherical dome, a resultant wrapping stress is generated and the element on the substrate would suffer severe deformation, degrading the optical performance of the microlens array. In order to reduce the wrapping stress and deformation, elastic polymer bridges⁶ are used to connect the microlens structures, as shown in Fig. 1(c). The polymer bridges were around 200 μm in thickness, and the microlenses structure were 450 μm thick. Owing to the difference in the thickness, most wrapping stress is distributed in the polymer bridges and thus the deformation of the microlenses is reduced.

The fabrication process was based on a soft lithography process,^{14,15} as illustrated in Fig. 2. Isobornyl acrylate (IBA) (Refs. 14 and 15) pre-polymer mixture was initially photopatterned under UV radiance (intensity, $I = 9 \text{ mW/cm}^2$; time, $t = 20 \text{ s}$) on a glass slide to form a 200 μm thick polymer mold, as shown in Fig. 2(a). Then another layer of IBA polymer was formed onto the patterned structures under UV radiance (intensity, $I = 9 \text{ mW/cm}^2$; time, $t = 20 \text{ s}$) to increase the height of the areas corresponding to the ultimate bridge structures to 400 μm , as shown in Fig. 2(b). Similar procedure was executed on a glass slide to form another mold, whose height was around 120 μm , for the fabrication of the aperture slip, as shown in Fig. 2(c). Then the IBA molds were transferred to polydimethylsiloxane (PDMS) to serve as the substrate and aperture slip, respectively. The liquid level of the PDMS mixture was lower than the IBA mold to form through-holes as the apertures. PDMS mixture was then cured on a hot plate at 65 °C for 4 h. Next, two fully cured PDMS layers were peeled off from the respective molds. After the inner surfaces of the cavities were treated from hydrophobic to hydrophilic by corona plasma discharge, two PDMS layers were bonded together,¹⁶ as shown in Fig. 2(d). Then NIPAAm precursor was injected into the cavities and

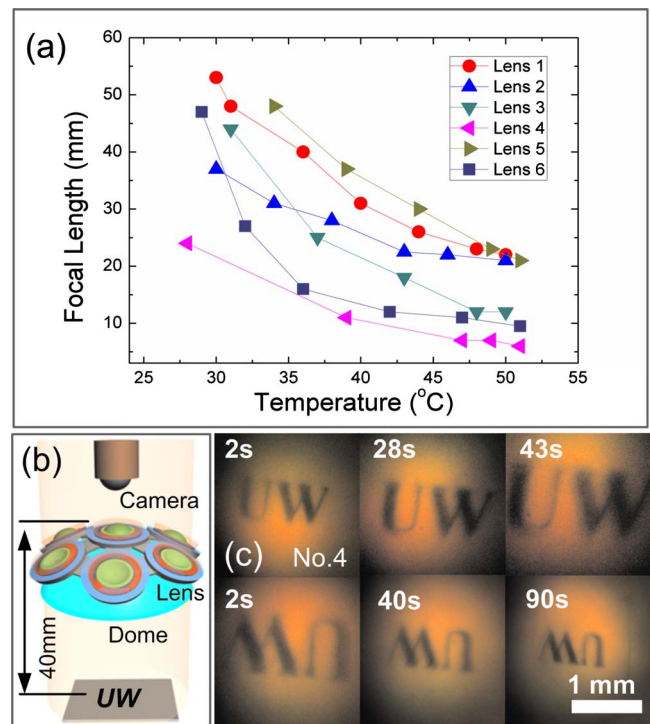


FIG. 3. (Color online) (a) Dynamic change in the focal length of each microlens, labeled in Fig. 1(c), at different temperatures. (b) Schematics of testing the imaging of the microlens array on the glass hemisphere. A transparency film with a logo of 1 mm tall UW was placed 22 mm below the glass dome. (c) Frame sequence of the focused images from one microlens (Number 4) in this microlens array in one scan. Initially, the microlens was convergent and real images were obtained. Owing to thermal dissipation, focal length of the microlens gradually increased, and thus the real images were magnified with time. Then the microlens switched to the divergent status, and the images were inverted as virtual images after being refocused. With further thermal dissipation, the negative focal length increased, resulting in the increase in size of the virtual images. The scale bar is 1 mm.

was photopatterned under UV light (intensity $I = 13.5 \text{ mW/cm}^2$; time $t = 8.5 \text{ s}$). Noncrosslinked hydrogel precursor was flushed away by ethanol and NIPAAm hydrogel rings were formed in the cavities. The sidewall of the aperture slip was treated by corona plasma discharge to hydrophilic to pin the water-oil menisci, as shown in Fig. 2(e). Next, this planar microlens array with soft PDMS substrate was wrapped onto a glass hemisphere with a diameter of 18 mm. Finally, each cavity was filled with water and covered by silicone oil, forming the water-oil interface. Separately fabricated PDMS barriers were used to keep the oil in the package, as shown in Fig. 2(f). The fabrication procedure of these PDMS barriers is not shown in the figure. The diameter of each microlens was 1.8 mm. Each cavity was 250 μm in depth and 4 mm in diameter. The shape of the original water-oil interface was determined by the volume of water filled.

Before the microlens array was wrapped onto a hemisphere, focal length of each microlens in the array was measured by determining the position of the optically minimum focused point of a collimated input light beam along the optical axis.¹⁷ A thermal resistor heater and the tip of a thermometer were placed under the microlens in order to control and measure the *in situ* surrounding temperature while the focused point of a microlens was being recorded. The dynamic focal lengths of the six microlenses at different temperatures ranging from 53 to 25 °C were obtained, as plotted in Fig. 3(a). The positive focal lengths of six microlenses

varied from 6 mm (1), 9 mm (2), 12 mm (3), 21 mm (4), 22 mm (5) and 21 mm (6), respectively, to infinity. The number of each microlens is labeled in Fig. 1(c). Nonuniformity stems from the nonuniformity in our exposure system when patterning the hydrogel actuators, as well as the various volume of water added into the individual cavity. The FOV of each lens was measured and to be from 77° to 128°, depending on the focal length of the lens.¹⁸

In the curvilinear microlens array fabricated on a dome, lenses are distributed on a spherical cap with an angle θ of about 116° as defined and shown in Fig. 2(f). Figure 3(b) shows the set-up to test the imaging of the fabricated tunable-focus microlens array. An object plane with a logo of “UW” was positioned 40 mm below this curvilinear microlens array (including the underlying hemispherical glass dome). A charge coupled device-coupled stereoscope was positioned above this microlens array to monitor and record images obtained from the microlenses and the dome. The microlens array wrapped on the dome was first heated to 55 °C on a hot plate. Then the microlens array was removed from the hot plate and placed under the stereoscope. As the hydrogel actuators in the microlenses were cooled down to the room temperature (25 °C) by thermal dissipation, images from the microlenses were recorded.

The frame sequence from the recorded video of one microlens (4) was shown in Fig. 3(c). Note that the hemispherical glass dome also contributed to the ultimate images. The magnification and inversion of the focused images were observed. Initially the microlens was convergent. During the recording process, the stereoscope was fine tuned to keep the images clear. With decreasing temperature, the focal length increased to infinity and the resulting image magnified. After the microlens switched from convergent to divergent, the inverted virtual images were obtained by moving the stereoscope along the optical axis. As the temperature decreases, the inverted images gradually shrunk, indicating an increase in the negative focal length.

In summary, we have demonstrated a curvilinear tunable-focus microlens array with six microlenses. Liquid-based microlens is connected through thin flexible PDMS bridges and is omnidirectionally fabricated on a transparent hemispherical dome. The microlenses are distributed on a cap subtending an angle of 116°. Each microlens is individually tuned by a thermo-responsive hydrogel actuator around it. The wrapping stress and the deformation were reduced by thin connecting bridges. The range of the focal length of each microlens in this array varied from millimeter to infin-

ity. In future studies, we will improve the uniformity of the lenses through better lithography systems and precise control of the volume of the water filled into the cavity. The curvilinear microlens array is expected to cover the whole sphere and could have a distributed angle approaching 360° for a large FOV. Metal resistive microheaters and thermal coupling microsensors could be fabricated below every single hydrogel ring to control the temperature locally. The crosstalk among the actuators could be reduced by a thermal insulating layer. Images from microlenses could be transmitted to a photodetector under the dome via integrated waveguides.⁷ Such a lens array could be potentially integrated with flexible optoelectronics as well.⁶

This work was supported by the Defense Advanced Research Projects Agency (Grant No. HR0011-08-1-0048), the National Science Foundation (Grant No. ECCS 0745000), and partly by the Wisconsin Institutes for Discovery and the Wallace H. Coulter Foundation. The authors thank Daming Cheng for discussions. This research utilized NSF-supported shared facilities at the University of Wisconsin-Madison.

¹K. Carlson, M. Chidley, K. B. Sung, M. Descour, A. Gillenwater, M. Follen, and R. Richards-Kortum, *Appl. Opt.* **44**, 1792 (2005).

²S. Kuiper and B. H. W. Hendriks, *Appl. Phys. Lett.* **85**, 1128 (2004).

³H. Ren and S. T. Wu, *Opt. Express* **16**, 2646 (2008).

⁴D. Y. Zhang, V. Lien, Y. Berdichevsky, J. Choi, and Y. H. Lo, *Appl. Phys. Lett.* **82**, 3171 (2003).

⁵J. W. Duparré and F. C. Wippermann, *Bioinspir. Biomim.* **1**, R1 (2006).

⁶H. C. Ko, M. P. Stoykovich, J. Z. Song, V. Malyarchuk, W. M. Choi, C. J. Yu, J. B. Geddes, J. L. Xiao, S. D. Wang, Y. G. Huang, and J. A. Rogers, *Nature (London)* **454**, 748 (2008).

⁷K.-H. Jeong, J. Kim, and L. P. Lee, *Science* **312**, 557 (2006).

⁸D. Radtke, J. W. Duparré, U. D. Zeitner, and A. Tünnermann, *Opt. Express* **15**, 3067 (2007).

⁹R. J. Jackman, J. L. Wilbur, and G. M. Whitesides, *Science* **269**, 664 (1995).

¹⁰R. Yang, W. Wang, and S. A. Soper, *Appl. Phys. Lett.* **86**, 161110 (2005).

¹¹S. Yang, G. Chen, M. Megens, C. K. Ullal, Y.-J. Han, R. Rapaport, E. L. Thomas, and J. Aizenberg, *Adv. Mater. (Weinheim, Ger.)* **17**, 435 (2005).

¹²L. Dong, A. K. Agarwal, D. J. Beebe, and H. Jiang, *Nature (London)* **442**, 551 (2006).

¹³X. Zeng and H. Jiang, *Appl. Phys. Lett.* **93**, 151101 (2008).

¹⁴A. K. Agarwal, D. J. Beebe, and H. Jiang, *J. Micromech. Microeng.* **16**, 332 (2006).

¹⁵A. K. Agarwal, S. S. Sridharamurthy, D. J. Beebe, and H. Jiang, *J. Microelectromech. Syst.* **14**, 1409 (2005).

¹⁶K. Haubert, T. Drier, and D. Beebe, *Lab Chip* **6**, 1548 (2006).

¹⁷X. Zeng and H. Jiang, *J. Microelectromech. Syst.* **17**, 1210 (2008).

¹⁸X. Zeng and H. Jiang, in *The 15th International Conference on Solid-State Sensors, Actuators and Microsystems (Transducers '09)* (Denver, Colorado, 2009).